Supplemental Figures

Methionine Deficiency Facilitates Antitumor Immunity by Altering m^{6}A Methylation of Immune Checkpoint Transcripts

Ting Li, Yue-Tao Tan, Yanxing Chen, Xiao-Jun Zheng, Wen Wang, Kun Liao, Hai-Yu Mo, Junzhong Lin, Wei Yang, Hai-Long Piao, Rui-Hua Xu, Huai-Qiang Ju

Figure S1

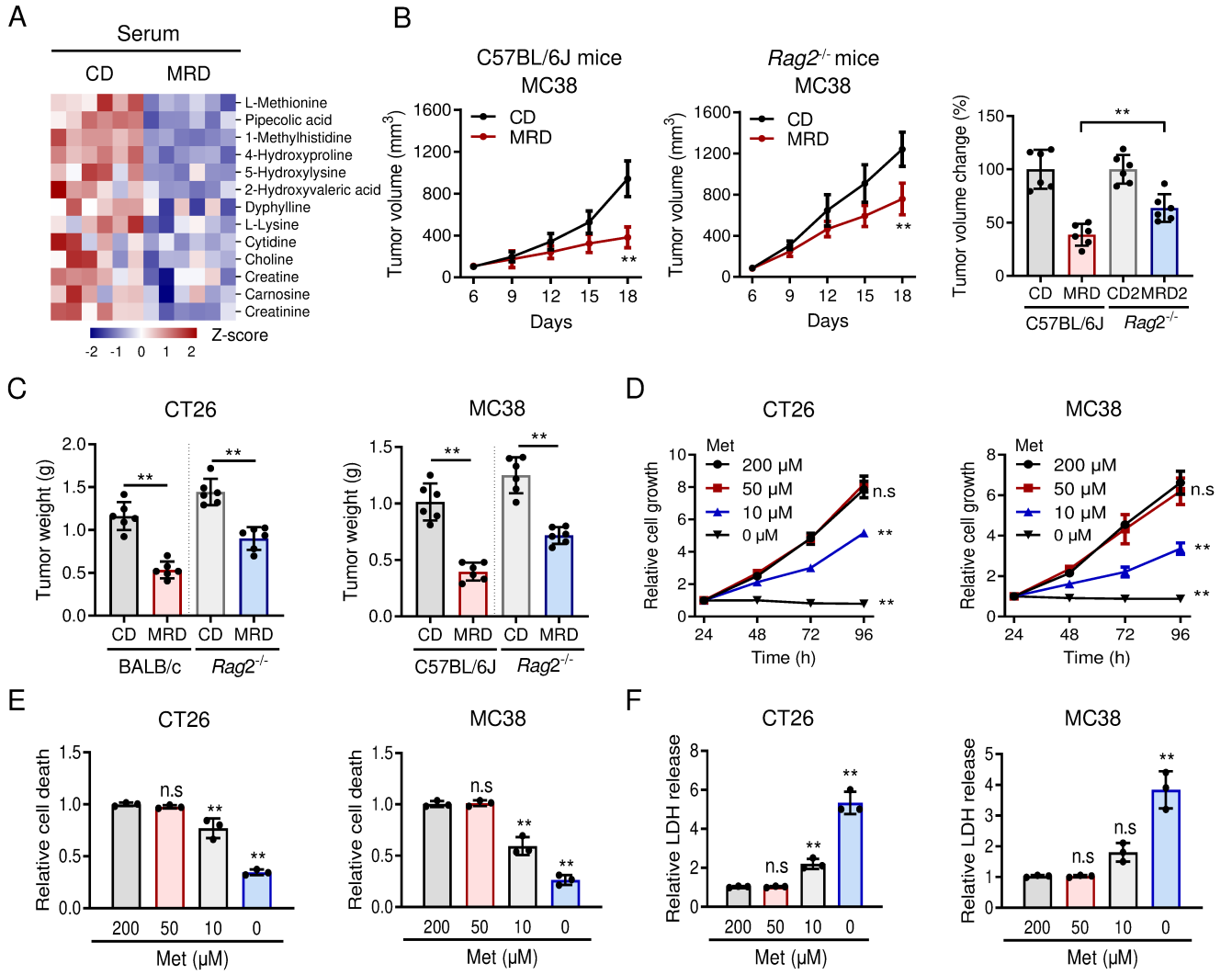

Figure S1. Methionine restriction suppressed tumor growth, related to Figure 1. (A) Heat map of changed metabolites in the serum of BALB/c mice and *Rag2*$^{-/-}$ mice implanted with CT26 cells and subjected to CD or MRD feeding. (n = 3 mice per group). **(B)** Subcutaneous tumor models established in C57BL/6J mice and *Rag2*$^{-/-}$ mice showing the tumor growth rate and growth rate change after implantation of MC38 cells with CD or MRD feeding. (n = 6 mice per group). **(C)** Subcutaneous tumor weight after implantation of CT26 (left) or MC38 (right) cells with CD or MRD feeding. (n = 6 mice per group). **(D-F)** MTS assays of the cell proliferation rate (D), flow cytometric analysis of cell death (E) and LDH assays of LDH release (F) of CRC cells with methionine-restricted or control medium treatment. The data in B-F are presented as the means ± SDs. *P* values were determined by two-way ANOVA (Tumor volume in **B** and **D**), one-way ANOVA (Tumor volume change in **B, E** and **F**) and two-tailed unpaired Student's *t* test (**C**) . $^{**}P < 0.01$; n.s, not significant.

Figure S2

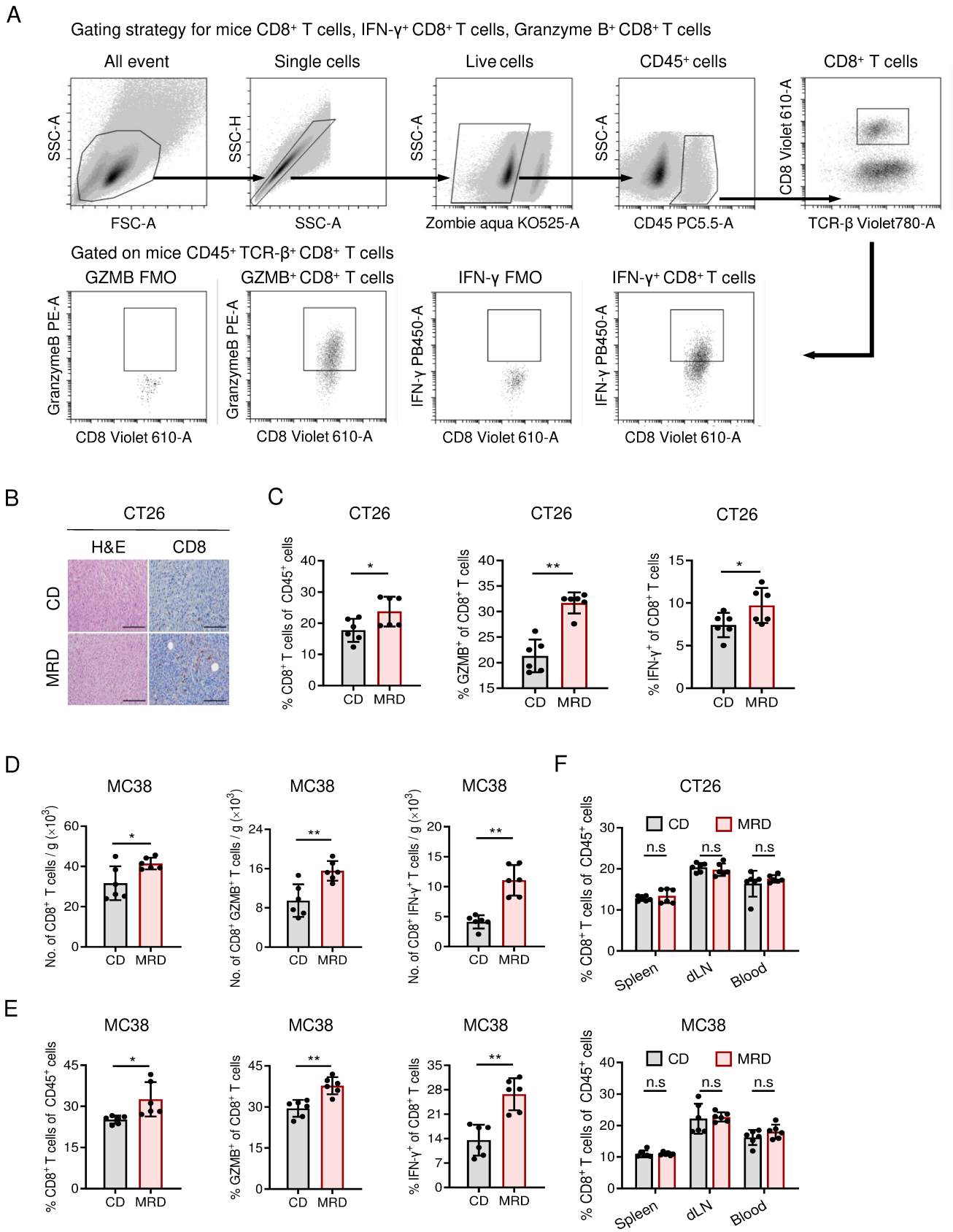
A
Gating strategy for mice CD8+ T cells, IFN-γ+ CD8+ T cells, Granzyme B+ CD8+ T cells
All event
Single cells
Live cells
CD45+ cells
CD8+ T cells
SSC-A
FSC-A
SSC-H
SSC-A
SSC-A
Zombie aqua KO525-A
SSC-A
CD45 PC5.5-A
CD8 Violet 610-A
TCR-β Violet780-A
Gated on mice CD45+ TCR-β+ CD8+ T cells
GZMB FMO
GZMB+ CD8+ T cells
IFN-γ FMO
IFN-γ+ CD8+ T cells
GranzymeB PE-A
CD8 Violet 610-A
IFN-γ PB450-A
B
CT26
H&E
CD8
CD
MRD
C
CT26
% CD8+ T cells of CD45+ cells
CT26
% GZMB+ of CD8+ T cells
CT26
% IFN-γ+ of CD8+ T cells
CD
MRD
D
MC38
No. of CD8+ T cells / g (×10^3)
MC38
No. of CD8+ GZMB+ T cells / g (×10^3)
MC38
No. of CD8+ IFN-γ+ T cells / g (×10^3)
E
MC38
% CD8+ T cells of CD45+ cells
MC38
% GZMB+ of CD8+ T cells
MC38
% IFN-γ+ of CD8+ T cells
F
CT26
% CD8+ T cells of CD45+ cells
n.s
Spleen
dLN
Blood
MC38
% CD8+ T cells of CD45+ cells

Figure S2

Figure S2. Methionine is critical for antitumor immunity via CD8$^+$ T cells, related to Figure 1. **(A)** Gating strategy for flow cytometric analysis. **(B)** Representative images of H&E and CD8 staining in subcutaneous tumor model mice implanted with CT26 cells and subjected to CD or MRD feeding (scale bar: 100 μm). **(C)** Flow cytometric analysis of the proportions of CD8$^+$ T cells, CD8$^+$ GZMB$^+$ T cells and CD8$^+$ IFN-γ$^+$ T cells in subcutaneous tumor model mice implanted with CT26 cells and subjected to CD or MRD feeding. (n = 6 mice per group). **(D-E)** Flow cytometric analysis of the number (D) and proportions (E) of CD8$^+$ T cells, CD8$^+$ GZMB$^+$ T cells and CD8$^+$ IFN-γ$^+$ T cells in subcutaneous tumor model mice implanted with MC38 cells and subjected to CD or MRD feeding. (n = 6 mice per group). **(F)** Flow cytometric analysis of the proportions of CD8$^+$ T cells in spleen, draining lymph nodes (dLN) and blood in subcutaneous tumor model mice implanted with CRC cells and subjected to CD or MRD feeding. (n = 6 mice per group). The data in C-F are presented as the means ± SDs. *P* values were determined by two-tailed unpaired Student's *t* test (**C-F**). **P* < 0.05; ***P* < 0.01; n.s, not significant.

Figure S3

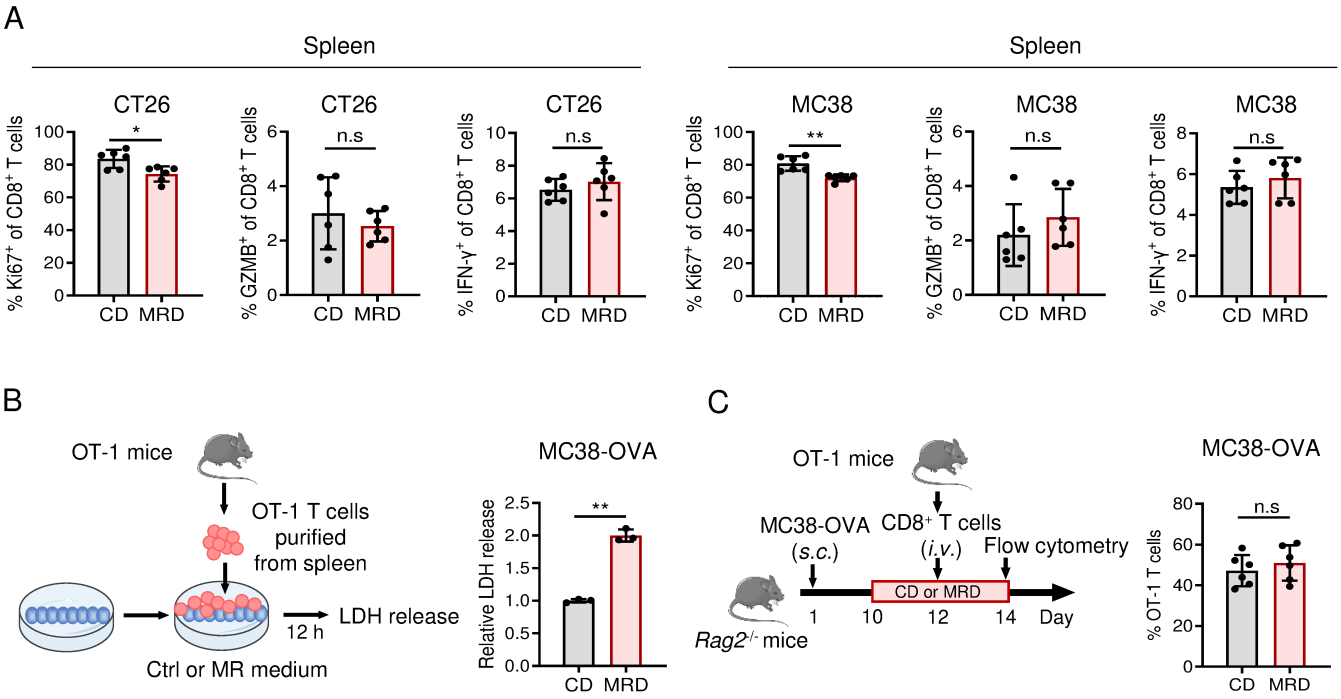

Figure S3. The effect of methionine restriction on CD8⁺ T cells, related to Figure 1. (A) Flow cytometric analysis of the proportions of CD8⁺ Ki67⁺ T cells, CD8⁺ GZMB⁺ T cells and CD8⁺ IFN-γ⁺ T cells in spleen in subcutaneous tumor model mice implanted with CRC cells and subjected to CD or MRD feeding. (n = 6 mice per group). **(B)** Experimental design for the CD8⁺ T cell cytotoxicity *in vitro* (left) and LDH release (right) with methionine-restricted or control medium treatment. **(C)** Experimental design for the CD8⁺ T cell infiltration *in vivo* (left) and flow cytometric analysis of the proportions of OT-1 T cells (right) in subcutaneous tumor model mice implanted with MC38-OVA cells upon CD or MRD feeding. (n = 6 mice per group). The data in A-C are presented as the means ± SDs. *P* values were determined by two-tailed unpaired Student's *t* test (**A-C**). **P* < 0.05; ***P* < 0.01; n.s, not significant.

Figure S4

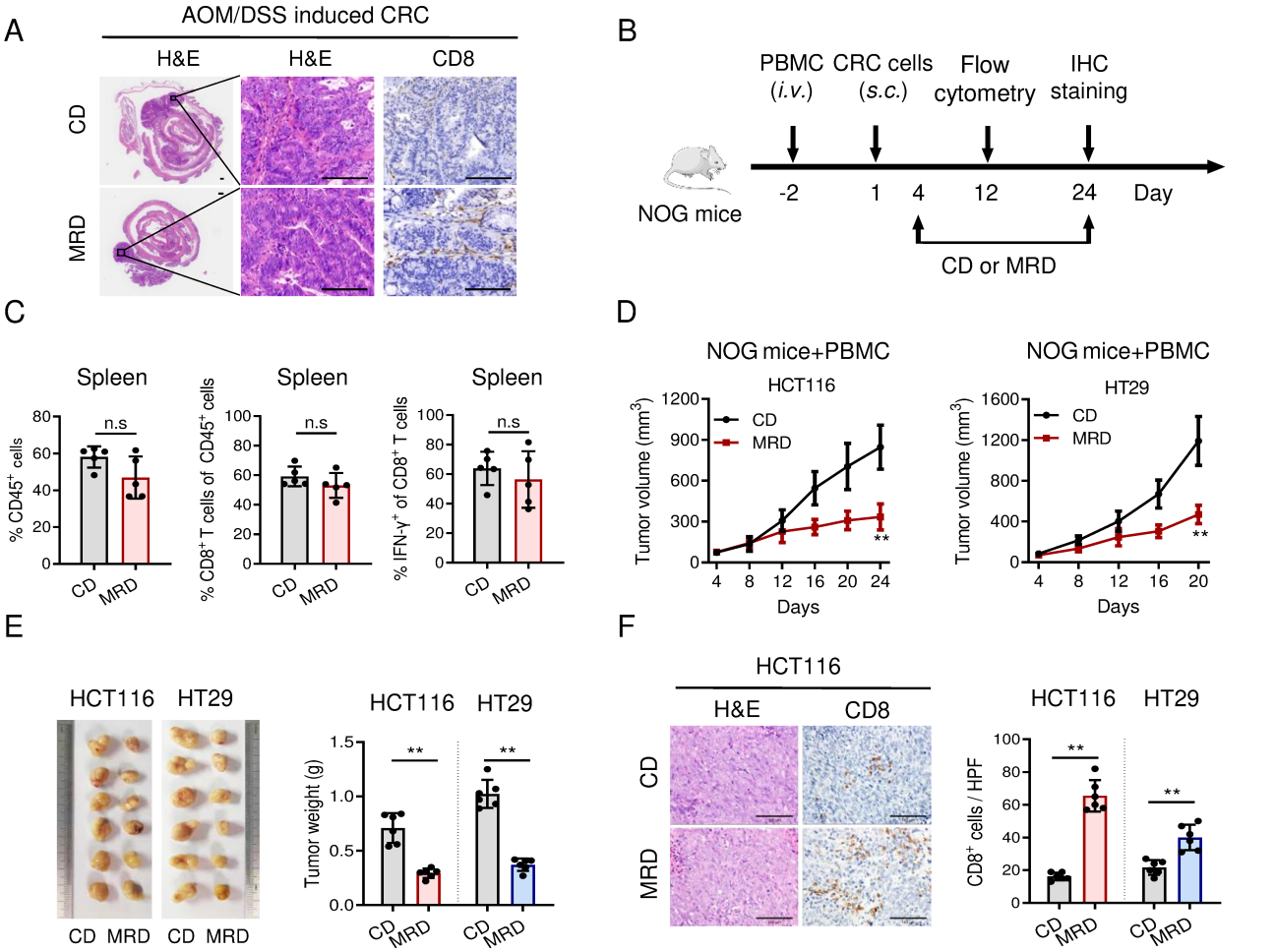

Figure S4. Experimental design and verification of AOM-DSS and humanized mouse model, related to Figure 1. (A) Representative images of H&E and CD8 staining in the spontaneous mouse colon cancer model with CD or MRD feeding (scale bar: 100 μm). **(B)** Experimental design for the HuPBMC reconstitution mouse model. **(C)** Flow cytometric analysis of the proportions of spleen $CD45^+$ immune cells, $CD8^+$ T cells and $CD8^+$ $IFN\text{-}\gamma^+$ T cells in the HuPBMC reconstitution mouse model with CD or MRD feeding. (n = 5 mice per group). **(D-E)** HuPBMC-reconstituted mouse model established in NOG mice showing the tumor growth rate (D) and tumor weight (E) after implantation of CRC cells with CD or MRD feeding. (n = 6 mice per group). **(F)** Representative images (left) and quantification (right) of H&E and CD8 staining in the HuPBMC-reconstituted mouse model with CD or MRD feeding. The data in C-F are presented as the means ± SDs. The *P* value was determined by two-tailed unpaired Student's *t* test (**C, E and F**) and two-way ANOVA (**D**). $^{**}P < 0.01$; n.s, not significant.

Figure S5

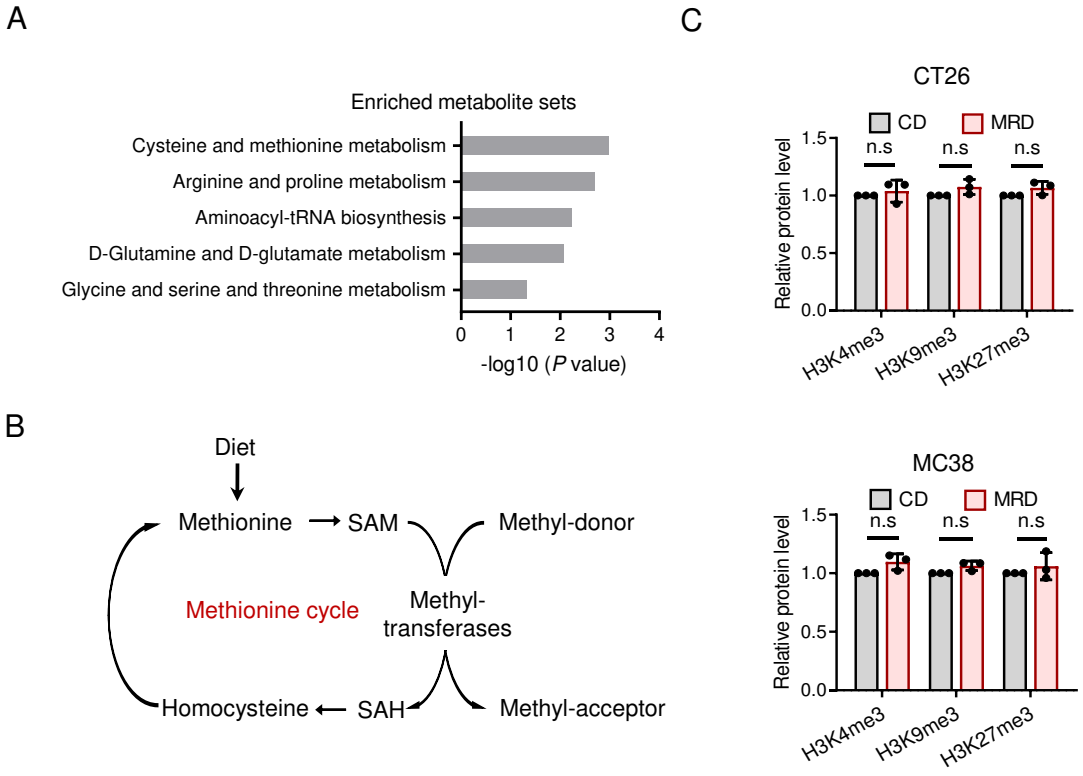

Figure S5. Methionine is essential for methyl transfer through converting to SAM, related to Figure 1. (A) Pathway analysis of altered metabolites in subcutaneous tumor model mice implanted with CT26 cells and subjected to CD or MRD feeding. **(B)** Schematic of methionine metabolism. **(C)** Quantification in immunoblotting of H3K4me3, H3K9me3 and H3K27me3 from subcutaneous tumors subjected to CD or MRD feeding. The data in C are presented as the means ± SDs. *P* values were determined by two-tailed unpaired Student's *t* test (**C**). n.s, not significant.

Figure S6

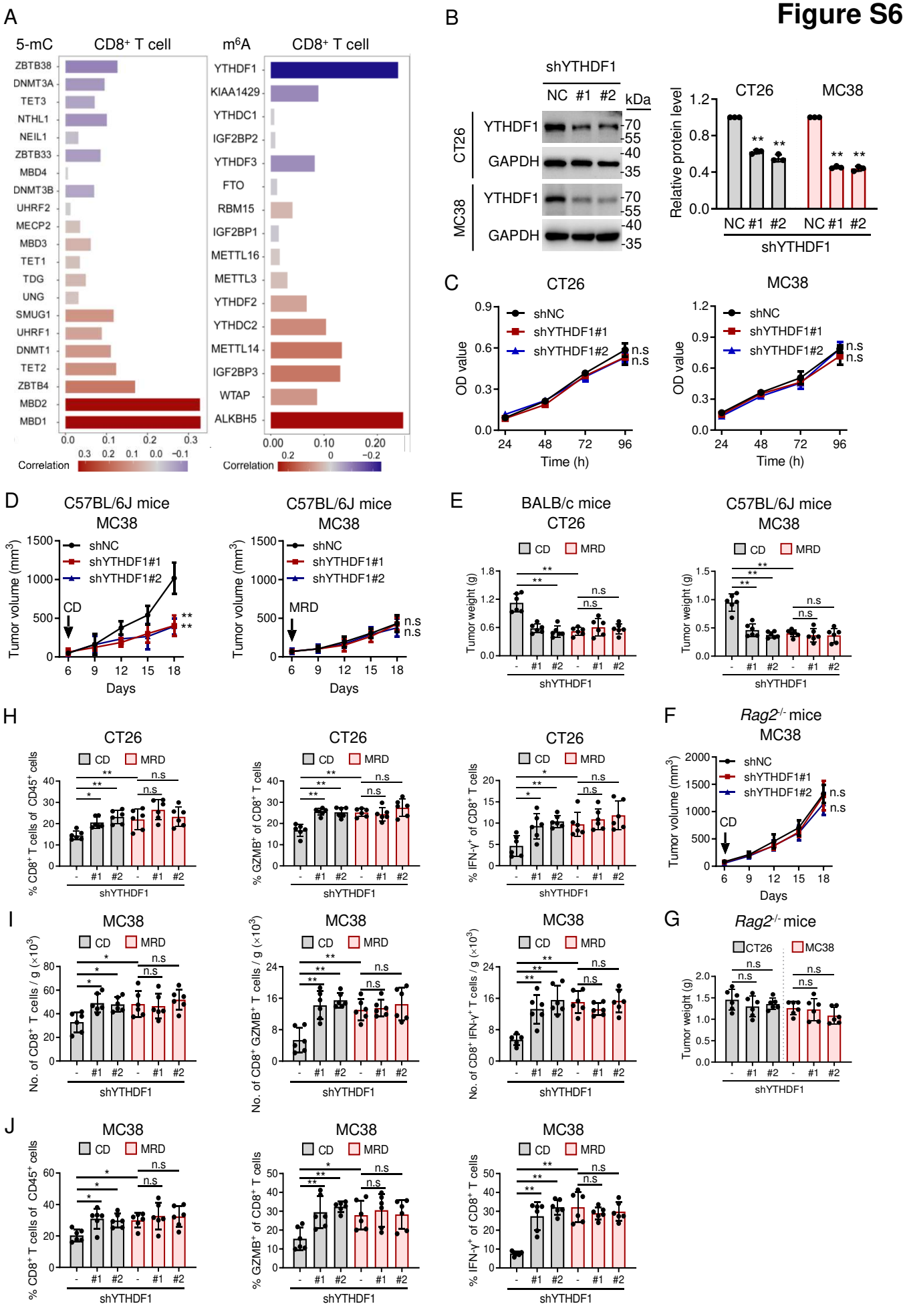
A
5-mC CD8+ T cell
m6A CD8+ T cell
ZBTB38
DNMT3A
TET3
NTHL1
NEIL1
ZBTB33
MBD4
DNMT3B
UHRF2
MECP2
MBD3
TET1
TDG
UNG
SMUG1
UHRF1
DNMT1
TET2
ZBTB4
MBD2
MBD1
YTHDF1
KIAA1429
YTHDC1
IGF2BP2
YTHDF3
FTO
RBM15
IGF2BP1
METTL16
METTL3
YTHDF2
YTHDC2
METTL14
IGF2BP3
WTAP
ALKBH5
Correlation
B
shYTHDF1
NC #1 #2
kDa
CT26
YTHDF1
GAPDH
MC38
Relative protein level
C
CT26
MC38
shNC
shYTHDF1#1
shYTHDF1#2
OD value
Time (h)
n.s
D
C57BL/6J mice
MC38
Tumor volume (mm3)
CD
MRD
Days
E
BALB/c mice
CT26
C57BL/6J mice
MC38
Tumor weight (g)
shYTHDF1
F
Rag2-/- mice
MC38
G
Rag2-/- mice
CT26
MC38
H
CT26
% CD8+ T cells of CD45+ cells
% GZMB+ of CD8+ T cells
% IFN-γ+ of CD8+ T cells
I
MC38
No. of CD8+ T cells / g (×10^3)
No. of CD8+ GZMB+ T cells / g (×10^3)
No. of CD8+ IFN-γ+ T cells / g (×10^3)
J
MC38
% CD8+ T cells of CD45+ cells
% GZMB+ of CD8+ T cells
% IFN-γ+ of CD8+ T cells

Figure S6

Figure S6. Methionine restriction enhances antitumor immunity via YTHDF1, related to Figure 2. (A) Correlations of the $CD8^+$ T cell infiltration with DNA 5-mC and RNA m^6A methylation regulators in CRC data from TCGA. **(B)** Immunoblotting (left) and quantification (right) of YTHDF1 in YTHDF1-knockdown cells. GAPDH was included as a loading control. **(C)** MTS assays of the cell proliferation rate of YTHDF1-knockdown and control cells. **(D)** Subcutaneous tumor models showing the tumor growth rate after implantation of YTHDF1-knockdown or control MC38 cells with CD (left) or MRD (right) feeding. (n = 6 mice per group). **(E)** Subcutaneous tumor weight after implantation of YTHDF1-knockdown or control cells with CD or MRD feeding. (n = 6 mice per group). **(F)** Subcutaneous tumor models showing the tumor growth rate after implantation of YTHDF1-knockdown or control MC38 cells in *Rag2*$^{-/-}$ mice. (n = 6 mice per group). **(G)** Subcutaneous tumor weight after implantation of YTHDF1-knockdown or control cells in *Rag2*$^{-/-}$ mice. (n = 6 mice per group). **(H)** Flow cytometric analysis of the proportions of $CD8^+$ T cells, $CD8^+$ $GZMB^+$ T cells and $CD8^+$ IFN-γ^+ T cells in subcutaneous tumor model mice implanted with YTHDF1-knockdown or control CT26 cells and subjected to CD or MRD feeding. (n = 6 mice per group). **(I-J)** Flow cytometric analysis of the number (I) and proportions (J) of $CD8^+$ T cells, $CD8^+$ $GZMB^+$ T cells and $CD8^+$ IFN-γ^+ T cells in subcutaneous tumor model mice implanted with MC38 cells and subjected to CD or MRD feeding. (n = 6 mice per group). The data in B-J are presented as the means ± SDs. *P* values were determined by one-way ANOVA (**B, E and G-J**) and two-way ANOVA (**C, D and F**). **P* < 0.05; ***P* < 0.01; n.s, not significant.

Figure S7

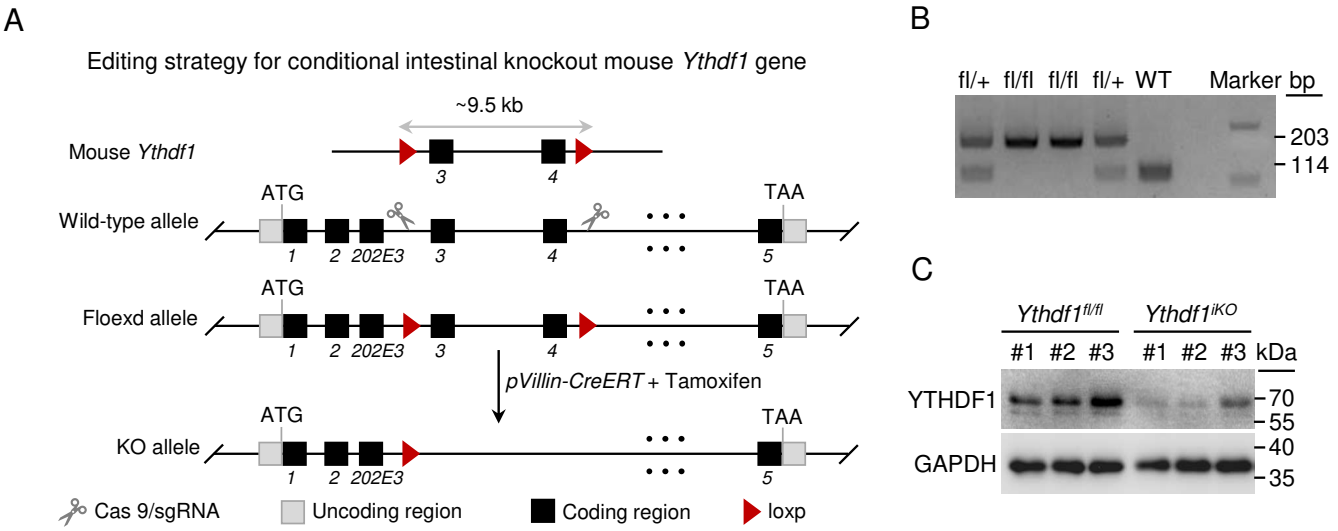

Figure S7. Experimental design and verification of AOM-DSS-induced mouse colon cancer model established in *Ythdf1*$^{fl/fl}$ and *Ythdf1*^{iKO} mice, related to Figure 2. (A) Editing strategy for conditional intestinal knockout of the mouse *Ythdf1* gene. Transgene expressing Cre recombinase under the control of the villin gene promoter (*villin-Cre-ERT2*), an intestine-specific promoter. **(B)** PCR genotyping using mouse tail DNA. PCR screening for *Ythdf1* revealed a band of 114 bp for the wild-type allele and a band of 203 bp for the floxed allele. **(C)** Immunoblotting of YTHDF1 in spontaneous tumors from *Ythdf1*$^{fl/fl}$ and *Ythdf1*^{iKO} mice after tamoxifen treatment. GAPDH was included as a loading control.

Figure S8

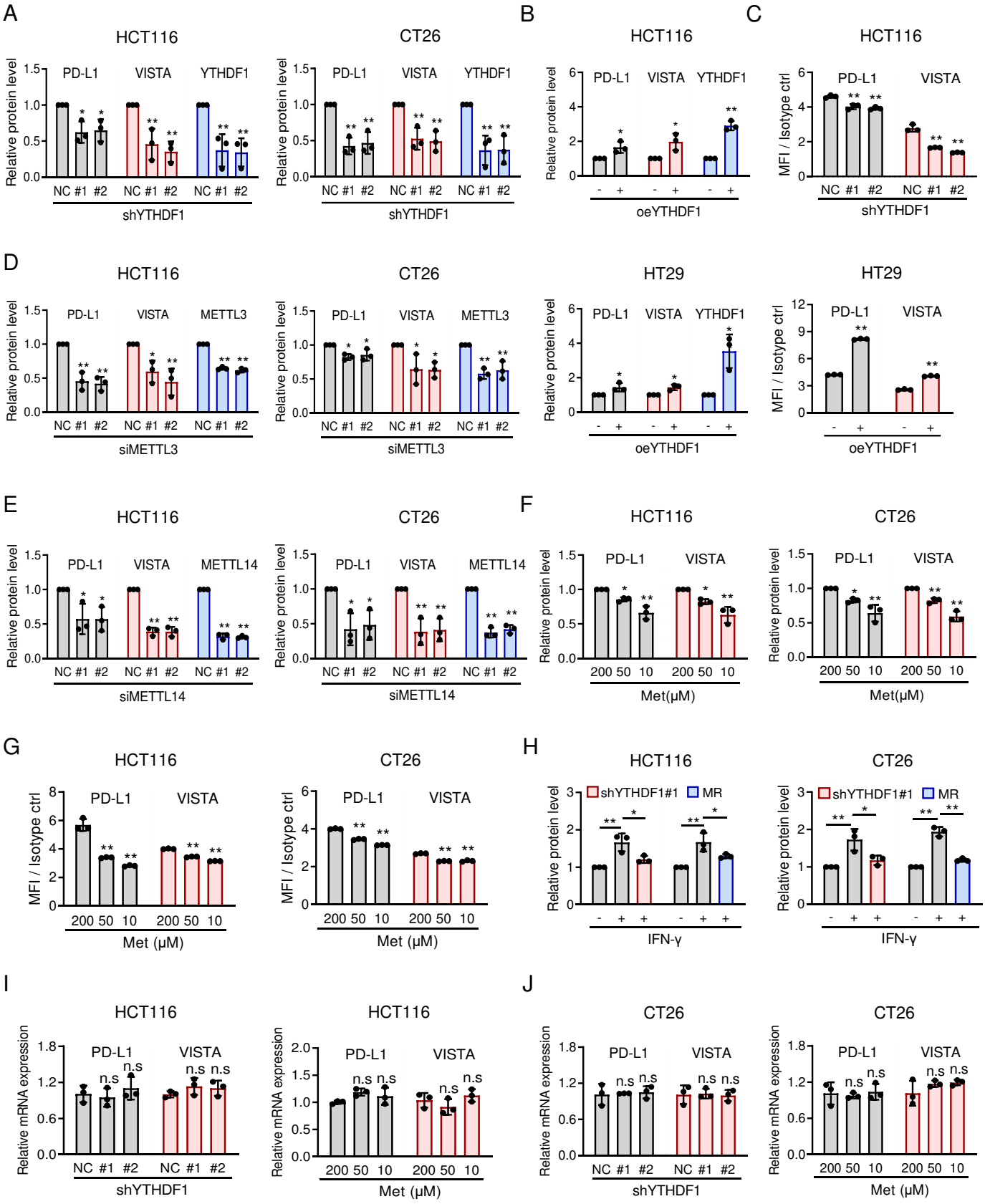
A
HCT116
CT26
PD-L1
VISTA
YTHDF1
Relative protein level
NC #1 #2
shYTHDF1
B
HCT116
oeYTHDF1
C
HCT116
MFI / Isotype ctrl
shYTHDF1
D
HCT116
CT26
METTL3
siMETTL3
HT29
oeYTHDF1
E
METTL14
siMETTL14
F
Met(μM)
200 50 10
G
Met (μM)
H
shYTHDF1#1
MR
IFN-γ
I
Relative mRNA expression
n.s
J

Figure S8

Figure S8. Methionine and YTHDF1 promote the translation of PD-L1 and VISTA, related to Figure 3. **(A-B)** Quantification in immunoblotting of PD-L1, VISTA and YTHDF1 after YTHDF1 inhibition (A) or YTHDF1 overexpression (B) in CRC cells. **(C)** Flow cytometric analysis of PD-L1 and VISTA after YTHDF1 inhibition in HCT116 cells (up) or YTHDF1 overexpression in HT29 cells (down). MFI, mean fluorence intensity. **(D)** Quantification in immunoblotting of PD-L1, VISTA and METTL3 after METTL3 inhibition in CRC cells. **(E)** Quantification in immunoblotting of PD-L1, VISTA and METTL14 after METTL14 inhibition in CRC cells. **(F-G)** Quantification in immunoblotting (F) and flow cytometric analysis (G) of PD-L1 and VISTA after methionine-restricted treatment in CRC cells. MFI, mean fluorence intensity. **(H)** Quantification in immunoblotting of PD-L1 after YTHDF1 inhibition with IFN-γ stimulation in CRC cells. **(I-J)** qPCR analysis of PD-L1 and VISTA expression after YTHDF1 inhibition (left) or methionine restriction (right) in HCT116 (I) and CT26 (J) cells. The data in A -J are presented as the means ± SDs. *P* values were determined by one-way ANOVA (**A,** HCT116 in **C** and **E-J**) and two-tailed unpaired Student's *t* test (**B** and HT29 in **C**). **P* < 0.05; ***P* < 0.01; n.s, not significant.

Figure S9

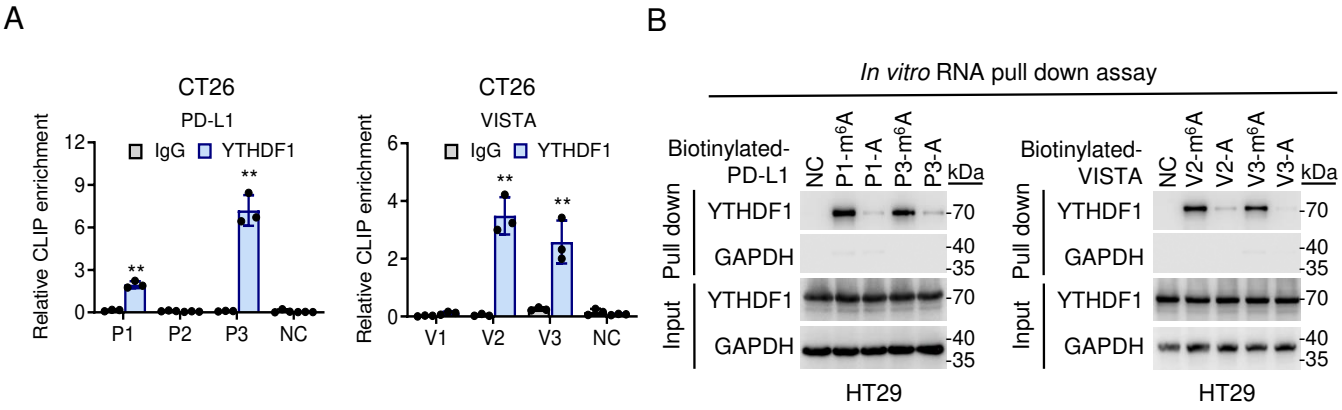

Figure S9. YTHDF1 regulates PD-L1 and VISTA expression in an m^{6}A-dependent manner, related to Figure 4. (A) CLIP-qPCR analysis of specific YTHDF1 binding enrichment in PD-L1 (left) and VISTA (right) mRNAs in CT26 cells. **(B)** *In vitro* RNA pull-down assays for YTHDF1 binding to biotinylated PD-L1 (left) probes or biotinylated VISTA (right) probes in HT29 cells. GAPDH was included as a loading control. The data in A are presented as the means ± SDs. The *P* value was determined by two-tailed unpaired Student's *t* test (**A**). $^{**}P < 0.01$.

Figure S10

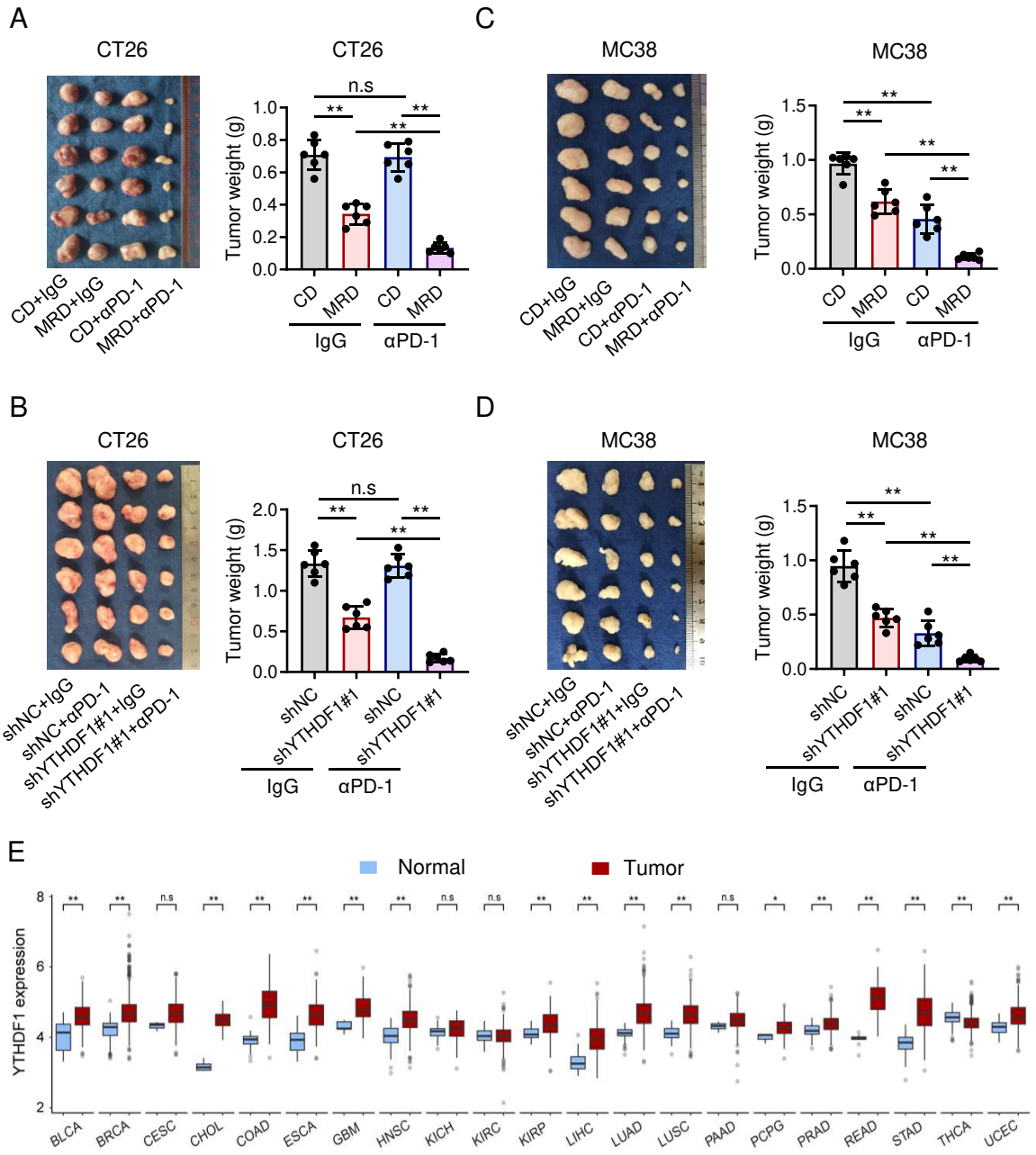

Figure S10. MRD or YTHDF1 depletion synergizes with PD-1 blockade, related to Figure 5. **(A)** CT26 subcutaneous tumor weight with CD or MRD feeding treated with IgG or αPD-1. (n = 6 mice per group). **(B)** Subcutaneous tumor weight with YTHDF1-knockdown or control CT26 cells treated with IgG or αPD-1. (n = 6 mice per group). **(C)** MC38 subcutaneous tumor weight with CD or MRD feeding treated with IgG or αPD-1. (n = 6 mice per group). **(D)** Subcutaneous tumor weight with YTHDF1-knockdown or control MC38 cells treated with IgG or αPD-1. (n = 6 mice per group). **(E)** Box plots of YTHDF1 expression in other TCGA cancer types. The data in A-D are presented as the means ± SDs. The data in E are presented as a box-and-whisker graph (min-max), and the horizontal line across the box indicates the median. *P* values were determined one-way ANOVA (**A-D**) and two-tailed unpaired Student's *t* test (**E**). **P* < 0.05; ***P* < 0.01. n.s, not significant.